Applied Physics Express **8**, 073002 (2015)
http://dx.doi.org/**10.7567/APEX.8.073002**

Current-induced dynamics of bubble domains in perpendicularly magnetized TbFeCo wires

Masaaki Tanaka[1*], Hiroki Kanazawa[1], Sho Sumitomo[1], Syuta Honda[2], Ko Mibu[1], and Hiroyuki Awano[3]

[1]*Graduate School of Engineering, Nagoya Institute of Technology, Nagoya 466-8555, Japan*
[2]*Faculty of Pure and Applied Sciences, University of Tsukuba, Tsukuba, Ibaraki 305-8573, Japan*
[3]*Information Storage Materials Laboratory, Toyota Technological Institute, Nagoya 468-8511, Japan*

Received March 25, 2015; accepted May 29, 2015; published online June 15, 2015

We investigated the bubble-domain dynamics in TbFeCo wires with perpendicular magnetization under electric current flows. In TbFeCo wires with relatively low saturation magnetization (M_s), the current pulse caused the bubble domains to collapse without moving. In TbFeCo wires with relatively high M_s, however, the bubble domains grew in the current direction. We explain these shape changes by assessing the M_s-dependent forces caused by the exchange field and magnetostatic field. We also found that we could control the current-induced behaviors of the bubble domains by using an external magnetic field.

Recently, there has been much interest in electric current-induced movements of magnetic domains or domain walls in magnetic wires in terms of their fundamental physics and their potential as new spintronics devices.[1–3] The magnetic domains of systems with perpendicular magnetic anisotropy have been predicted to move at low current densities because of their thinner domain walls and their more efficient spin-transfer torque than in in-plane magnetization systems,[4] and several experimental approaches have been reported so far.[5–8] However, when a domain wall forms across both wire edges, the edge roughness sometimes affects the domain wall movement.[4] Such unstable domain wall pinning is an issue to be solved for the domain wall movement. Bubble domains (BDs), used for magnetic-bubble memory and magneto-optical disks,[9,10] are also interesting in terms of both spintronics applications and fundamental research. They can be generated in perpendicularly magnetized films, and their domain walls do not reach the wire edges, and so they are expected to be drivable without influence from the edge roughness.

In this study, we investigated the BD dynamics in perpendicularly magnetized wires with different saturation magnetizations (M_s) exposed to current flow. For the perpendicularly magnetized material, we used TbFeCo, an amorphous rare-earth transition-metal alloy and a kind of speri-magnet.[9] In TbFeCo, the magnetic moment of Tb takes on a random cone arrangement whose net magnetization direction is opposite that of Fe and Co. Because of this opposition, the magnitude of saturation magnetization can be adjusted by changing the alloy composition. We found that the current-induced BD dynamics depended on the magnitude of M_s and that it was caused by differences in the effective forces acting on the BD walls from the exchange field, as well as on the magnetostatic field. We also controlled the current-induced BD dynamics using an external perpendicular magnetic field.

Using electron-beam lithography and lift-off, we fabricated 10-μm-wide and 80-μm-long TbFeCo wires with electric pads on both sides on thermally oxidized Si substrates. 10-nm-thick TbFeCo layers with 2-nm-thick Pt cap layers were grown by sputtering. The Pt layers protected the wires from oxidization. We prepared TbFeCo wires of two different compositions whose saturation magnetizations were 40 and 200 emu/cm^3. Polar Kerr hysteresis loops showed that the magnetization of each sample was on the transition-metal-dominant side. Current pulses with durations of 10 ms were applied to the wires. Joule heating in the TbFeCo wires was negligible under the conditions of the present study.[11] To directly observe the current-induced BD dynamics, we used polar-magneto-optical Kerr effect (MOKE) microscopy in differential imaging modes. In the figures here, the white and black regions in the magnetic wires correspond to the upward and downward magnetized regions, respectively. Figure 1 shows a MOKE micrograph of a BD in the TbFeCo wire and an illustration of the current-induced measurements. The BDs were generated in the wires as follows.[12] First, a magnetic field of more than 3 kOe was applied upward and perpendicular to the substrate plane in order to align the magnetization of the wires in one direction. The centers of the TbFeCo wires were heated for 0.5 s using a 407-nm laser at 8 mW with a magnetic field of approximately 1 kOe applied downward and perpendicular to the substrate plane. This produced a downward magnetized BD at the center of each TbFeCo wire. Subsequently, we adjusted the diameters of the BDs to approximately 2 μm by using a perpendicular magnetic field without heating. Using MOKE microscopy, we found that the laser heating caused no permanent damage to the wires.

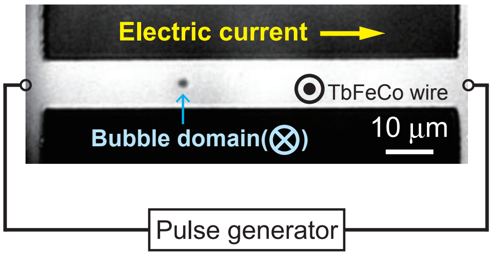

Fig. 1. A magneto-optical Kerr micrograph of a BD in a TbFeCo wire and an illustration of the experimental setup.

Figure 2(a) shows the BD dynamics of a TbFeCo wire with $M_s = 40$ emu/cm^3 for a single current pulse (2.0×10^{10} A/m^2) without an external magnetic field. Under this current, the BD collapsed instantly. Through further experiments, we found that BDs collapsed from this current flow in TbFeCo wires with $M_s = 40$–60 emu/cm^3. In contrast, in the TbFeCo wire with $M_s = 200$ emu/cm^3, the BD grew in the current direction at a threshold current density of 4.6×10^{10} A/m^2 without an external magnetic field, as shown in Fig. 2(b). The right edge of the BD expanded with an oblique angle after 30 pulses, whereas the left edge was pinned at the original position. The BDs in the TbFeCo wires with $M_s =$ 150–200 emu/cm^3 grew in the direction of the current flow (i.e., opposite the electron flow). Several groups have claimed that the reverse or transverse forces with respect to the

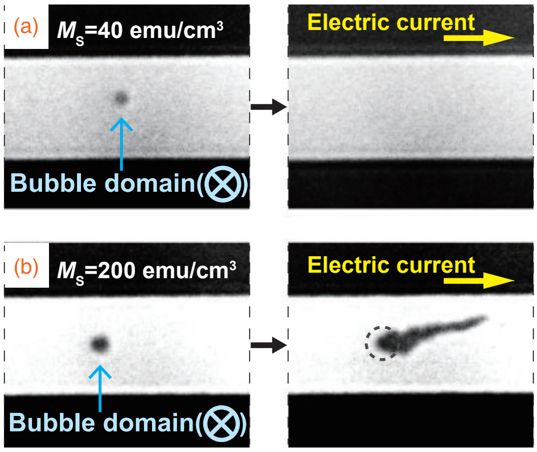

Fig. 2. Magneto-optical Kerr micrographs of the current-induced effect on the BDs in TbFeCo wires. The changes are shown in TbFeCo wires with (a) $M_s = 40\,\mathrm{emu/cm^3}$ after application of one current pulse at 2.0×10^{10} $\mathrm{A/m^2}$ and (b) $M_s = 200\,\mathrm{emu/cm^3}$ after application of 30 current pulses at $4.6 \times 10^{10}\,\mathrm{A/m^2}$.

electron flow can act on the usual magnetic domains and domain walls in perpendicular magnetic wires by the Rashba effect, the Dzyaloshinskii–Moriya (DM) interaction, or the spin Hall effect of the Pt cap layer.[13–18)]

We also investigated current-induced BD dynamics in the TbFeCo wires with $M_s = 200\,\mathrm{emu/cm^3}$ by applying perpendicular magnetic fields (H_{bias}). Here, we define downward H_{bias} as the positive field. Figures 3(b)–3(d) are MOKE micrographs showing the current-induced effect for BDs in TbFeCo wires in a magnetic field of −200 Oe with one current-pulse injection, in −20 Oe with five current-pulse injections, and in +200 Oe with one current-pulse injection. Applying H_{bias} of −20 Oe perpendicular to the plane produced stable BD movement by a current flow, as shown in Fig. 3(c). These results clarify that the current-induced BD dynamics can be controlled by H_{bias}. Figure 3(a) shows how the threshold current density, i.e., the lowest current density needed to change the BD shape, depended on H_{bias} in TbFeCo wires with $200\,\mathrm{emu/cm^3}$. By applying H_{bias} downward and perpendicular to the plane, the BDs grew in the current direction. As the magnitude of H_{bias} increased, the threshold current density decreased. By applying negative H_{bias} under −100 Oe, the BDs collapsed instantly with the current pulse.

We performed micromagnetic calculations of the current-induced BD dynamics in a nanowire with perpendicular magnetic anisotropy based on the Landau–Lifshitz equation.[19,20)]

$$\frac{\partial \boldsymbol{m}}{\partial t} = -|\gamma|\boldsymbol{m} \times \boldsymbol{H}_{\mathrm{eff}} - \alpha|\gamma|[\boldsymbol{m} \times (\boldsymbol{m} \times \boldsymbol{H}_{\mathrm{eff}})] - \frac{\boldsymbol{m} \times (\boldsymbol{m} \times \nabla j_s)}{M_s}, \qquad (1)$$

where $\boldsymbol{m}$ is a unit vector along the local magnetic moment of each small cell and γ is the gyromagnetic constant of $-1.76 \times 10^7\,\mathrm{rad/(s{\cdot}Oe)}$. The magnetization ($M_s$) was set to 40, 100, or $120\,\mathrm{emu/cm^3}$ and the damping constant (α) was set to 0.1. The effective magnetic field ($\boldsymbol{H}_{\mathrm{eff}}$) is a combination of the static, exchange, and uniaxial magnetic anisotropy fields. The exchange magnetic field was calculated by using the exchange stiffness constant (A) of $1.0 \times 10^{-8}\,\mathrm{erg/cm}$.

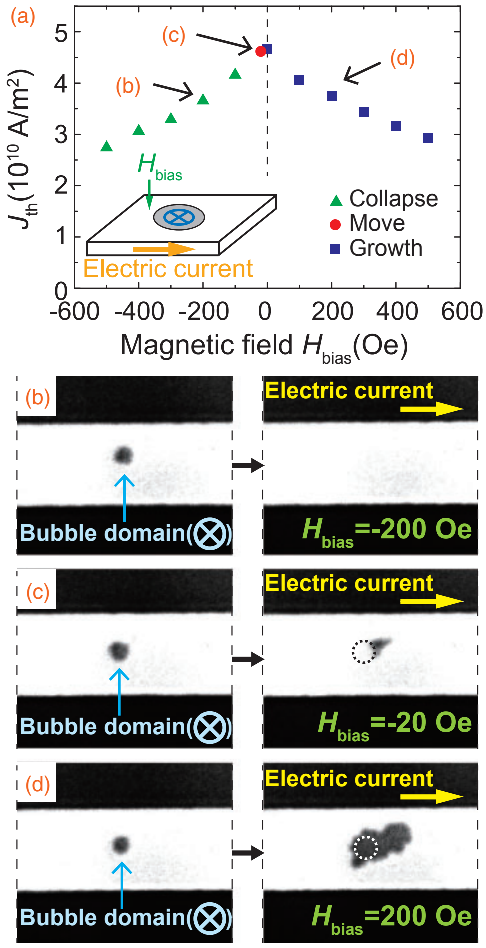

Fig. 3. (a) Dependence of the threshold current density, J_{th} (for BD shape change), on the perpendicular magnetic field in TbFeCo wires with 200 $\mathrm{emu/cm^3}$. The inserted figure shows the experimental setup. Also shown are MOKE micrographs showing the effect of current on the BDs in TbFeCo wires with magnetic fields of (b) −200 Oe after one current-pulse injection, (c) −20 Oe after five current-pulse injections, and (d) +200 Oe after one current-pulse injection. The dotted circles show the initial positions of the BDs.

A perpendicular anisotropy energy (K_u) of $1.0 \times 10^5\,\mathrm{erg/cm^3}$ was used to estimate the magnetic anisotropy field, which is perpendicular to the plane of the wire. We calculated the spin-polarized current density (j_s) from a current of $-2.0 \times 10^{11}\,\mathrm{A/m^2}$ and a spin polarization (P) of 0.5. The sizes of the small cell and the wire were $5 \times 5 \times 5\,\mathrm{nm^3}$ and $500 \times 200 \times 10\,\mathrm{nm^3}$, respectively. The initial BD diameter was set to approximately 35 nm. We could not reproduce the current-induced BD dynamics in calculations using the K_u and A parameters reported in the literature,[21)] possibly because the speri-magnet TbFeCo is assumed to be a ferromagnet. Because of this inconsistency, we tuned the parameters to give reasonable results; the current-induced BD dynamics must be calculated in a system close to the experimental conditions. With this in mind, we simulated the time dependence of the BD shape for films with different values of M_s under continuous DC current. Figure 4(a) shows the initial BD state, in which the magnetic moments around the domain wall tilt slightly. In these simulations, we set the initial BDs to have smaller areas than those in the experiments, and so these simulations show the M_s dependence of the current-induced BD dynamics over a short time scale. Figures 4(b),

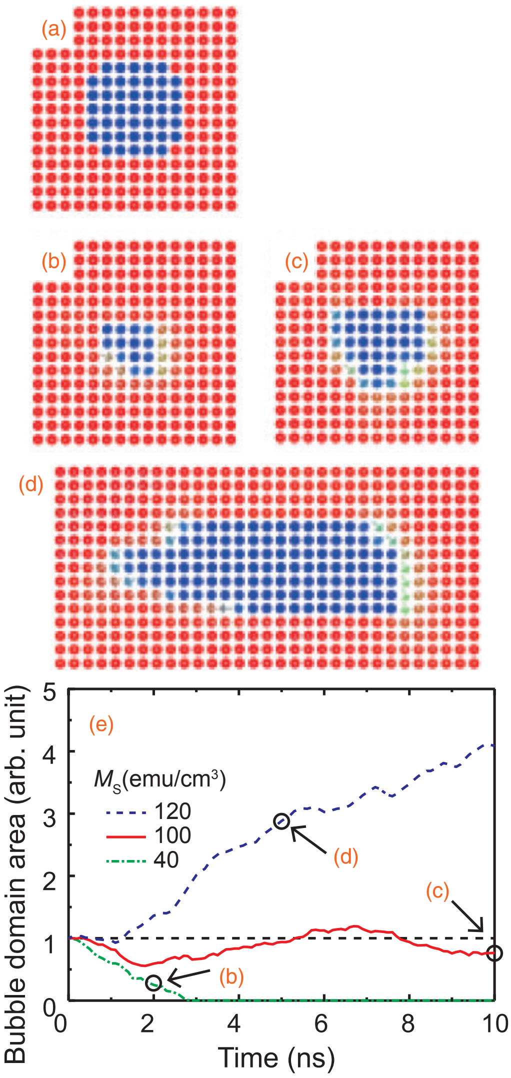

Fig. 4. Time dependence of the current-induced BD dynamics from the micromagnetic calculation. BD shapes are shown for (a) the initial state, (b) the film with $M_s = 40\,\mathrm{emu/cm^3}$ after 2 ns, (c) the film with $M_s = 100\,\mathrm{emu/cm^3}$ after 10 ns, and (d) the film with $M_s = 120\,\mathrm{emu/cm^3}$ after 5 ns. (e) Time dependence of the BD area in a DC current flow for different values of M_s.

4(c), and 4(d) show the calculated results of the BD shape without an external magnetic field in the film with $M_s = 40\,\mathrm{emu/cm^3}$ after 2 ns, in the film with $M_s = 100\,\mathrm{emu/cm^3}$ after 10 ns, and in the film with $M_s = 120\,\mathrm{emu/cm^3}$ after 5 ns. Figure 4(e) is the time dependence of the BD area in continuous current flow for magnetic wires with different values of M_s. In the magnetic wires with $M_s = 40\,\mathrm{emu/cm^3}$, the simulated BD disappeared while moving in the electron flow direction. In the wire with $M_s = 120\,\mathrm{emu/cm^3}$, the simulated BD grew while moving in the electron flow direction. In the wire with $M_s = 100\,\mathrm{emu/cm^3}$, however, the simulated BD moved in the electron flow direction while maintaining its area. All calculated BDs moved in the electron direction, which conflicts with the experimental results. This difference occurred because the calculation did not consider the reverse or transverse forces from the Rashba effect, the DM interaction, or the spin Hall effect of the Pt cap layer. The point in this simulation is that the M_s-dependent BD-shape changes are quantitatively consistent with the experimental results.

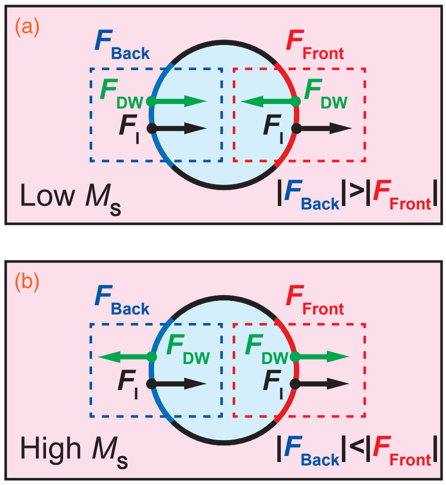

Fig. 5. Schematics of the total force acting on the rigid front end ($\boldsymbol{F}_{\mathrm{Front}}$) and the rigid back end ($\boldsymbol{F}_{\mathrm{Back}}$) of the domain walls of the BDs for films with (a) low and (b) high saturation magnetization. $\boldsymbol{F}_{\mathrm{Front}}$ and $\boldsymbol{F}_{\mathrm{Back}}$ include the current-induced force ($\boldsymbol{F}_{\mathrm{I}}$) and the M_s-dependent force ($\boldsymbol{F}_{\mathrm{DW}}$).

Based on our results, we propose a simple model for BD shape changes in films with different values of M_s in Fig. 5. In this model, we assume that the torque acting on the magnetic moments of a domain wall produces an effective in-plane force acting perpendicular to the domain wall of the BD. We also assume that the domain wall was moved by this effective force regardless of domain wall type. We consider a current-induced effective force ($\boldsymbol{F}_{\mathrm{I}}$) and an M_s-dependent force ($\boldsymbol{F}_{\mathrm{DW}}$). $\boldsymbol{F}_{\mathrm{Front}}$ and $\boldsymbol{F}_{\mathrm{Back}}$, shown in Fig. 5, are the sum of $\boldsymbol{F}_{\mathrm{I}}$ and $\boldsymbol{F}_{\mathrm{DW}}$ for the front and back ends, respectively. The front and back ends of the BDs are assumed to be rigid. The current-induced effective force ($\boldsymbol{F}_{\mathrm{I}}$) is defined as the sum of the effective force caused by the spin-transfer torque, the DM interaction, the Rashba effect, and the spin Hall effect. The M_s-dependent force ($\boldsymbol{F}_{\mathrm{DW}}$) includes the forces induced by the exchange field and the magnetostatic field.[22] The exchange-field-induced force compresses the BDs because the exchange energy decreases as the BD radius decreases. The magnetostatic-field-induced force, which decreases as the BD area increases, expands the BDs. When $\boldsymbol{F}_{\mathrm{DW}}$ is smaller than the threshold force needed to change the BD shape, the BD holds its shape. For the BDs in films with low M_s, the magnetostatic-field-induced force is small, and so the exchange-field-induced force dominates in $\boldsymbol{F}_{\mathrm{DW}}$. Thus, $\boldsymbol{F}_{\mathrm{DW}}$ for the BDs acts toward the BD center, as shown in Fig. 5(a). In films with low M_s, $\boldsymbol{F}_{\mathrm{DW}}$ at the back end acts in the same direction as $\boldsymbol{F}_{\mathrm{I}}$ and $\boldsymbol{F}_{\mathrm{DW}}$ at the front end acts in the opposite direction of $\boldsymbol{F}_{\mathrm{I}}$. Thus, $\boldsymbol{F}_{\mathrm{Front}}$ becomes smaller than $\boldsymbol{F}_{\mathrm{Back}}$, and the back end moves by lower current density than the front end. In films with high M_s, the magnetostatic-field-induced force is larger than that in films with low M_s, so $\boldsymbol{F}_{\mathrm{DW}}$ acts toward the outside of the BD, as shown in Fig. 5(b). Thus, in these films, the threshold current density of front-end movement is lower than that of the back-end movement. Because of these differences in front- and back-end forces, the BD shape varied in films with different saturation magnetizations.

In summary, we investigated current-induced BD dynamics in TbFeCo wires with different saturation magnetizations. We found that the M_s-dependent forces, which include the exchange-field-induced force and the magnetostatic-field-induced force, affected the current-induced BD dynamics. We also found that the current-induced behavior of the BDs can be controlled by applying an external perpendicular magnetic field.

Acknowledgments This work was supported by JSPS KAKENHI Grant Numbers 25820135, 24656219, and 24360126. This work was also supported by the Nanotechnology Platform Program (Nagoya Institute of Technology and Toyota Technological Institute) of the Ministry of Education, Culture, Sports, Science and Technology, Japan.

1) A. Yamaguchi, T. Ono, S. Nasu, K. Miyake, K. Mibu, and T. Shinjo, Phys. Rev. Lett. **92**, 077205 (2004).
2) M. Yamanouchi, D. Chiba, F. Matsukura, and H. Ohno, Nature **428**, 539 (2004).
3) M. Hayashi, L. Thomas, C. Rettner, R. Moriya, Y. B. Bazaliy, and S. S. P. Parkin, Phys. Rev. Lett. **98**, 037204 (2007).
4) S.-W. Jung, W. Kim, T.-D. Lee, K.-J. Lee, and H.-W. Lee, Appl. Phys. Lett. **92**, 202508 (2008).
5) H. Tanigawa, T. Koyama, G. Yamada, D. Chiba, S. Kasai, S. Fukami, T. Suzuki, N. Ohshima, N. Ishiwata, Y. Nakatani, and T. Ono, Appl. Phys. Express **2**, 053002 (2009).
6) S. Li, H. Nakamura, T. Kanazawa, X. Liu, and A. Morisako, J. Magn. Soc. Jpn. **34**, 333 (2010).
7) D. Chiba, G. Yamada, T. Koyama, K. Ueda, H. Tanigawa, S. Fukami, T. Suzuki, N. Ohshima, N. Ishiwata, Y. Nakatani, and T. Ono, Appl. Phys. Express **3**, 073004 (2010).
8) D.-T. Ngo, K. Ikeda, and H. Awano, Appl. Phys. Express **4**, 093002 (2011).
9) T. Suzuki, *Magneto-Optical Recording Materials* (Wiley, New York, 2000) p. 5.
10) R. J. Gambino, J. Magn. Soc. Jpn. **15**, S1_1 (1991).
11) M. Kawamoto, D. Bang, and H. Awano, Ext. Abstr. Int. Symp. Physics of Magnetic Materials (ISAMMA 2013), QD-09.
12) T. Ogasawara, N. Iwata, Y. Murakami, H. Okamoto, and Y. Tokura, Appl. Phys. Lett. **94**, 162507 (2009).
13) I. M. Miron, T. Moore, H. Szambolics, L. D. Buda-Prejbeanu, S. Auffret, B. Rodmacq, S. Pizzini, J. Vogel, M. Bonfim, A. Schuhl, and G. Gaudin, Nat. Mater. **10**, 419 (2011).
14) T. Suzuki, S. Fukami, N. Ishiwata, M. Yamanouchi, S. Ikeda, N. Kasai, and H. Ohno, Appl. Phys. Lett. **98**, 142505 (2011).
15) T. Koyama, H. Hata, K.-J. Kim, T. Moriyama, H. Tanigawa, T. Suzuki, Y. Nakatani, D. Chiba, and T. Ono, Appl. Phys. Express **6**, 033001 (2013).
16) D. Bang and H. Awano, Appl. Phys. Express **5**, 125201 (2012).
17) S.-G. Je, D.-H. Kim, S.-C. Yoo, B.-C. Min, K.-J. Lee, and S.-B. Choe, Phys. Rev. B **88**, 214401 (2013).
18) O. Boulle, S. Rohart, L. D. Buda-Prejbeanu, E. Jué, I. M. Miron, S. Pizzini, J. Vogel, G. Gaudin, and A. Thiaville, Phys. Rev. Lett. **111**, 217203 (2013).
19) Z. Li and S. Zhang, Phys. Rev. B **70**, 024417 (2004).
20) S. Honda and T. Kimura, JPS Conf. Proc. **5**, 011017 (2015).
21) M. T. Rahman, X. Liu, and A. Morisako, IEEE Trans. Magn. **41**, 2568 (2005).
22) A. H. Bobeck, Bell Syst. Tech. J. **46**, 1901 (1967).